Applicability of isothermal three-parameter equations of state of solids—a reappraisal

2005 J. Phys.: Condens. Matter 17 6193

(http://iopscience.iop.org/0953-8984/17/39/007)

INSTITUTE OF PHYSICS PUBLISHING JOURNAL OF PHYSICS: CONDENSED MATTER

J. Phys.: Condens. Matter **17** (2005) 6193–6216 doi:10.1088/0953-8984/17/39/007

Applicability of isothermal three-parameter equations of state of solids—a reappraisal

Papiya Bose Roy[1] **and Sushil Bose Roy**

Department of Chemistry, T. M. Bhagalpur University, Bhagalpur–812007, India

E-mail: papiya_boseroy@rediffmail.com

Received 16 May 2005, in final form 4 August 2005
Published 16 September 2005
Online at stacks.iop.org/JPhysCM/17/6193

Abstract

The objective of the present study, an extension of a recent one, is to inter-compare the utility of the various isothermal three-parameter equations of state (EOSs) of solids, considered viable at different stages in the development of the EOS field, spanning over a period of about a century now. In a recent paper we have compared our isothermal three-parameter equation of state of solids with seven three-parameter isothermal EOSs—five corresponding to the regression curves of V/V_0 on P, and two to those of P on V/V_0. In this study, we investigate the relative utility of 21, i.e., virtually all, of the viable three-parameter EOSs—for the purposes of smoothing and interpolation of pressure–volume data, and extraction of accurate values of isothermal bulk modulus and its pressure derivative—corresponding to the regression curves of P on V/V_0. We have applied the EOSs, with no constraint on the parameters, to accurate and model-independent isotherms of nine solids, and assessed the goodness of the fitting accuracy; goodness of the stability of the fit parameters B_0, B_0', and B_0'' with variation in the pressure/compression ranges; and goodness of the agreement of the fit parameters B_0 and B_0' with experiment. Further, an additional test of goodness of randomization of the data points about the fit curves, quantified in terms of the number of wiggles of the data deviation curves about the fits, is also applied in the present study. The EOSs subjected to these seven tests are the three-parameter extensions of the EOS models formulated by Bridgman (1929), Murnaghan (1937), Birch (1938), Slater (1939), Davis and Gordon (1967), Macdonald (1969), Holzapfel (1991), Poirier and Tarantola (1998), and the so-called 'universal EOS' promoted by Vinet *et al* (1986). Also included for the inter-comparison purposes are the three-parameter EOSs proposed by Keane (1954), Mao (1970), Thomsen (1970), Huang and Chow (1974), Luban (1983), Freund and Ingalls (1989), Kumari and Dass (1990), Hama and Suito (1996), and Bose Roy and Bose Roy (1999), and also the EOS based on a modified Eulerian strain as suggested by Sushil *et al* (2004). Interestingly, the three-parameter Mie–Gruneisen EOS, built on the

[1] Author to whom any correspondence should be addressed.

century-old Mie potential (Partington 1957, Stacey and Davis 2004), is also tested. The present study leads to some remarkable findings. Most notably, some of the old EOS models like those of Birch and of Keane, and also the Mie–Gruneisen EOS, are observed to be in better agreement with experiment than most of the EOSs that appeared much later in the literature. An inter-comparison of the overall results inferred from all the 21 EOSs—based on the most stringent discrimination technique comprising seven important tests ever applied in the literature—demonstrates that, while most of the EOSs marginally differ from each other constituting a narrow band of applicability, our model is decisively superior to all of them.

(Some figures in this article are in colour only in the electronic version)

1. Introduction

A precise knowledge of the interatomic forces at the stress-free state and their variation with pressure and temperature would help, in principle, not merely to calculate all the thermodynamic properties of a substance, but rather also address the problems related to a large part of physics—because almost all physical phenomena, discarding the world inside the atomic nucleus, may be attributed directly or indirectly to the forces between atoms. A lack of such a precise knowledge has prompted the proposition of a large number of isothermal two- and three-parameter empirical equations of state (EOSs), over a period of over a century now [1–44], all of them claiming a successful representation of the experimental EOS data. However, more often than not, the capability of these EOSs in describing the compressional behaviour of materials at high pressures has been discussed with little or no reference to the existing EOSs, and thus the relative utility of the existing EOSs continues to be a point of speculation.

A few comments may be made here, with regard to the functional form, terminology, and validity of an EOS. In the literature, namely [28], an isothermal EOS, $P = f(V/V_0)$, in which pressure is the dependent and volume is the independent variable, is labelled as 'non-inverted'; and an EOS $V/V_0 = f(P)$, with volume as the dependent and pressure as the independent variable, is called an 'inverted' EOS. These terminologies are incorrect and misleading on semantic grounds—it would be appropriate to label the former as the 'inverted', or better still, as the 'unrealistic', and the latter as the 'non-inverted' or 'realistic' EOS. In the present study we compare all the EOSs considered, corresponding to the regression curves of P on V/V_0, i.e., the unrealistic form, because EOSs in the unrealistic forms are readily amenable to thermodynamic manipulations. Strictly speaking, all such isothermal EOSs, which are explicitly expressible in the unrealistic forms only, can be readily dismissed, should a physical and logical basis be insisted on, as their very functional forms imply that the change in volume is the 'cause' and the change in pressure is the 'effect'—an assertion which is in utter conflict with the experimental position, i.e., Nature. That they offer a theoretical advantage of being readily amenable to thermodynamic manipulations, unlike the realistic forms, is an inadequacy of the thermodynamic frame. Realistic forms, however, have some intrinsic advantages [36, 44, 60]. Further, the validity of an EOS does not depend on the rationale on which EOSs are formulated, i.e., whether the EOSs are empirical, or whether they are having a theoretical basis, and to what extent the underlying theoretical bases are appealing to, or in conformity with, the existing theoretical knowledge. Furthermore, the validity of an EOS is

also not dependent on how best it responds to the theoretical boundary conditions [44]. The only necessary and sufficient condition for the validity of an EOS, within the confines of the aimed purposes, is its agreement with experiment. Of course, an EOS founded on a theoretical basis, and exhibiting a similar or better behaviour with experiment than an empirical one, within the confines of the experimental purposes for which it is designed and tested, is definitely more useful because of its flexibility for wider applications. About four decades ago, Hayard [86] emphasized that 'Many attempts have been made to derive a compressibility equation from molecular theory, but none of them has resulted in a convenient equation expressing the results of experiments with adequate accuracy. To meet this need it is necessary to employ some empirical equation, the sole justification for which is that it works'—and this position remains unchanged even to date. It may sound strange, but it is not, because one cannot discount the fact that the modern physics is founded on a mere empirical fitting.

There are two pathways for the inter-comparative study, either by using the measured values of the bulk modulus as inputs, or by curve-fitting. In an ideal situation, when error-free compression and bulk modulus data are available, and a perfectly well behaved equation of state is also available, the input of the bulk modulus data in such an EOS will generate the ideal compression data. On the other hand, the EOS on fitting with the ideal compression data will reproduce the ideal set of bulk modulus data used as inputs. Thus there will be a perfect synchronization between the two approaches. However, we do not have, at the moment, an unambiguous set of bulk modulus data even for a solid as simple as NaCl [37] and as stable as Cu, as discussed later. Furthermore, the experimental uncertainty, accompanying the measured bulk modulus values, in general, is much larger than those for the measured isotherms. It may be appreciated that the ambiguity with regard to conclusion on the adequacy of an EOS, in the case of the 'input' approach, is much higher compared to that based on the curve-fitting technique. Conceivably, there are two distinct situations, for accurate EOS data, in which a good agreement between the data curve and fit may be achieved in the 'input' approach. First, the systematic biases, that invariably bear a sign, arising from the poor functional form of the EOS tend to cancel the systematic biases resulting from the constraints imposed by the ambiguous set of bulk modulus data as well as the additional constraints of the interrelation between them. In fact, a number of authors have exploited this possibility by choosing a particular set of bulk modulus data that best suits to enforce the validity or utility of their models. Second, because the EOS behaves well, and the resultant of the systematic biases related to the bulk modulus data is reduced to an insignificant level, due to cancellation effects—statistically, however, such situations of mutual cancellation effects are highly improbable. Further, although an observed disagreement beyond experimental uncertainty may be attributed to the systematic biases inherent in the EOS model as well as the bulk modulus data, it is also possible that the EOS behaves well otherwise, but is forced to follow a deviant path due to the highly uncertain bulk modulus data. Obviously, under such situations, individual identification of the EOS bias is not possible. This is why, agreement or disagreement, either way it is difficult to arrive at a conclusion on the adequacy of an EOS. While in the curve-fitting approach, if the EOS data are accurate, the deviations in the predictions may be attributed mainly to the poor functional form of the EOS model, because a well optimized EOS resists a deviant path [87]. Therefore, if the EOS data are accurate and model independent, and range to large pressure/compression values, the curve fitting is the correct approach to assess or compare the prediction capability of an EOS. An obsession of various workers with the appropriateness of the 'input' approach [17, 45, 46, 50, 70, 80], over the decades, in conjunction with the paucity of the experimentally measured values of B_0'', has, in fact denied the three-parameter EOSs as much attention as the two-parameter EOSs, in respect of their utility. However, the traditionally accepted view that the inclusion of increasing number of parameters would

increasingly improve the behaviour of an EOS towards experiments is not necessarily true, for reasons referred to in [37]. Sometimes the authors, viz [47], obsessed with the 'input' approach, but confronted with the problem of selection of data, picked up a measured value of B_0 of their choice, and treated B_0' as a fitting parameter to achieve the best fit to the higher-pressure EOS curves. This approach is also unjustified because of the inherent interdependence of the bulk modulus values.

An EOS plays an important role in the physics of condensed matter. It helps us to predict ground-state bulk properties [83], mechanical properties of materials in our surroundings under extreme conditions, as in geological formations and settings [81] and for numerous industrial applications [82, 84]. Our goal in this study is to investigate the relative utility of virtually all the viable isothermal three-parameter EOSs, on the basis of a stringent discrimination technique comprising seven important tests—for the purposes of smoothing and interpolation of pressure–volume data, and extraction of accurate values of isothermal bulk modulus and its pressure derivative—corresponding to the regression curves of P on V/V_0.

2. Empirical equations of state

Here only the isothermal three-parameter EOSs are presented for consideration. Constancy of temperature is assumed throughout, and no special notation is used. V and V_0 are the volumes at pressure P and zero, respectively, while B_0, B_0', and B_0'' are the isothermal bulk modulus and their pressure derivatives in the stress-free state.

A potential function of the general form based on the century-old potential (1903) proposed by Mie and extended by Gruneisen [79] is

$$E(r) = -A(a/r)^m + B(a/r)^n.$$

Here, a is the equilibrium (zero-pressure) value of atomic spacing, r. A, and B are positive constants with the dimensions of energy, and m and n are dimensionless indices ($n > m$), often, but not necessarily, integers.

The three-parameter EOS built on this well known potential [41], and hereafter referred to as the Mie–Gruneisen EOS, is

$$P = \{3B_0/(n-m)\}[(V/V_0)^{-(1+n/3)} - (V/V_0)^{-(1+m/3)}] \tag{1}$$

where

$$n = 3[(1/2)(B_0'^2 + 4B_0B_0'')^{1/2} + (1/2)B_0' - 1],$$

$$m = 3[(1/2)B_0' - 1 - (1/2)(B_0'^2 + 4B_0B_0'')^{1/2}] \quad \text{and} \quad (n-m) = 3(B_0'^2 + 4B_0B_0'')^{1/2}.$$

It may be noted here that a number of EOSs have appeared in the literature where m and n are regarded as disposable parameters with specific choices—to illustrate, the well known two-parameter Born–Mie EOS is a special case, with $m = 1$. Further, it will be interesting to note that the three-parameter EOS, purported to be based on the generalized Lennard-Jones potential, by Sun (equation (4) of [44]), is the same as the Mie–Gruneisen EOS formulated above.

Murnaghan's [3] two-parameter EOS is based on a Taylor expansion of the isothermal bulk modulus to second order in terms of the pressure. Murnaghan himself, however, realized the inadequacy of this two-parameter EOS at high compression, and proposed a three-parameter EOS to include B_0'' [6], which can be put in the unrealistic form as

$$P = B_0[\{2(V/V_0)^{\Gamma} - 2\}/\{B_0'(1 - (V/V_0)^{\Gamma}) - \Gamma(1 + (V/V_0)^{\Gamma})\}], \tag{2}$$

with

$$\Gamma^2 = B_0'^2 - 2B_0B_0'' > 0.$$

Birch [7, 9–11] developed an expression based on the Eulerian strain measure $f = [(V_0/V)^{2/3} - 1]/2$. A Taylor expansion of the strain energy in terms of f, truncated at the fourth-order term of energy in strain, yields the following three-parameter EOS:

$$P = 3B_0 f(1+2f)^{5/2}[1 + a_1 f + a_2 f^2 + \cdots], \tag{3}$$

with

$$a_1 = 3/2(B_0' - 4) \qquad \text{and} \qquad a_2 = 3[B_0 B_0'' + B_0'(B_0' - 7) + (143/9)]/2.$$

This equation is, in fact, the three-parameter extension of the two-parameter EOS that has achieved prominence in the literature as the Birch–Murnaghan EOS through its application by Birch [7–10] and others to problems of finite compression in the interior of the earth. It was apparently first written by Murnaghan [3] in an early exposition of the thoughts which led eventually to his 1951 treatise [17].

Birch [10] using Murnaghan's finite elasticity theory has shown that at pressures existing in the earth's interior the gradient of the bulk modulus B with pressure P is a decreasing function of pressure. Keane [13] noted that an exact solution of a formula, from a derivation of Murnaghan [5], for the calculation of B and $\mathrm{d}B/\mathrm{d}P$ at large pressures is impossible to obtain, without the knowledge of the variation of the bulk modulus with pressure. This recognition prompted Keane [14] to come up with an improved Murnaghan model with an explicit use of the equation of state parameter B_∞', the asymptotic limit of B' as $P \to \infty$.

$$P = B_0[(B_0'/B_\infty')((V/V_0)^{-a} - 1) + ((B_0'/B_\infty') - 1)\ln(V/V_0)]. \tag{4}$$

Here,

$$a = B_\infty'.$$

Davis and Gordon [15] chose to expand the pressures in powers of V_0/V, about $V_0/V = 1$ or $V = V_0$. This expansion, up to the cubic term, leads to a three-parameter EOS:

$$P = B_0[(x-1) + (1/2)(B_0' - 1)(x-1)^2 + (1/6)(B_0'^2 - 3B_0' + 2 + B_0 B_0'')(x-1)^3], \tag{5}$$

where

$$x = V_0/V.$$

Mao [18] derived an empirical equation of state for high compression from the assumption that $B(\mathrm{d}P/\mathrm{d}B) = a + bP$, where a and b are constants determined by the initial conditions. Successive integration of this equation leads to

$$P = (a/b)\{[1 - (B_0(b-1)/a)\ln(V/V_0)]^{b/(b-1)} - 1\}, \tag{6}$$

where

$$a = B_0/B_0' \qquad \text{and} \qquad b = 1 - (B_0 B_0''/B_0')^2 \neq 1.$$

This straightforward modification of the Murnaghan model reduces to the two-parameter Murnaghan EOS for $b = 1$.

Huang and Chow [20] proposed a relatively simple three-parameter EOS which may be expressed in the unrealistic form as

$$P = (1/b)[\{1 - (1/a)(1 - (V/V_0))\}^{-(1/c)} - 1], \tag{7}$$

with

$$a = (1 + B_0')/(1 + B_0' + B_0 B_0''), \qquad b = (B_0'/B_0) - [B_0''/(B_0' + 1)]$$
$$\text{and} \qquad c = (1 + B_0' + B_0 B_0'')/(B_0'^2 + B_0' - B_0 B_0'').$$

An improved version of the Murnaghan model, proposed by Luban [22] and extensively used by Anderson *et al* [22], can be explicitly expressed in the realistic form only, as

$$V/V_0 = \exp\{(-1/\alpha^2 B_0)[\alpha\beta P + (\alpha - \beta)\ln(1 + \alpha P)]\}, \tag{8}$$

with

$$B_0' = B_0(\alpha - \beta) \qquad \text{and} \qquad B_0'' = -2\beta B_0'.$$

Vinet *et al* [24] strongly promoted a two-parameter EOS proposed by Rose *et al* [23], founded on the well known Rydberg empirical potential function, as the so-called universal EOS. This EOS was in fact first proposed earlier by Stacey [21, 85] and rediscovered by Rose [41]. The three-parameter extension of this model yields the following EOS [27]:

$$P = 3B_0(1 - x)(x^{-2})(\exp M). \tag{9}$$

Here,

$$M = (3/2)(B_0' - 1)(1 - x) + (3/2)(1 - x)^2[(1/4)B_0'^2 + (1/2)B_0' + B_0 B_0'' - (19/36)]$$
$$\text{and} \qquad x = (V/V_0)^{1/3}.$$

Freund and Ingalls [28] modified the 'usual' Tait equation [37], which may be put in the unrealistic form as

$$P = (1/b)[\exp\{(1/a)(1 - (V/V_0)^{1/c})\} - 1], \tag{10}$$

with the parameters

$$a = [(B_0'^2 - 4B_0B_0'')^{1/2} - B_0']/[(B_0'^2 - 4B_0B_0'')^{1/2} + B_0'],$$
$$b = [(B_0'^2 - 4B_0B_0'')^{1/2} + B_0']/2B_0 \qquad \text{and} \qquad c = 2[(B_0'^2 - 4B_0B_0'')^{1/2} - B_0'].$$

Kumari and Dass [29] presented an improved version of the Murnaghan equation by taking the high-order terms in the Taylor series expansion into account, on the basis of the assumption of the constancy of the ratio $B_0^{(n+1)}/B_0^{(n)} = B_0''/B_0'$ for $n > 1$, with $B_0^{(n)}$ as the n th-order pressure derivative of the isothermal bulk modulus at zero pressure. Their EOS, expressed explicitly in the unrealistic form, is

$$P = (-B_0'/B_0'')[\ln\{(m + ((V/V_0)^{-n}))/(1 + m)\}]. \tag{11}$$

Here,

$$m = -B_0'^2/B_0B_0'' \qquad \text{and} \qquad n = B_0' - (B_0B_0''/B_0').$$

Holzapfel [30] proposed an EOS, labelled as the HO_2 relation, in the form

$$P = 3B_0(V/V_0)^{-(n/3)}(1 - (V/V_0)^{1/3})[\exp\{(1.5B_0' + 1/2 - n)(1 - (V/V_0)^{1/3})\}], \tag{12}$$

where

$$n = 5.$$

A choice of $n = 2$ in the above relation would correspond to the so-called two-parameter universal equation of state of solids [24]. This relation has been used in recent years to determine the EOS of some solids [68, 76]. Recently Kunc *et al* [77] noted that the best least-squares fit for describing their theoretical pressure–volume data for diamond was achieved with $n = 7/2$. This value yields an EOS which is a blend of the Vinet form and the Holzapfel expression. Obviously, the specific choice of n yields a specific EOS. In the present study we have regarded n as a free parameter in curve fitting, thus converting the above HO_2 relation into a three-parameter EOS.

Hama and Suito [34] have examined some EOSs for solids by comparing them with the theoretical results calculated by the augmented-plane-wave method and quantum statistical

model (QSM) proposed by Kalitkin and Kuzmina [34 and citations therein]. For the application to polyatomic solids, they implanted into the linearized scheme of Vinet *et al* [24] the results from the QSM solution and formulated a modified three-parameter universal EOS

$$P = 3B_0 x^{-5}(1-x)\exp[(3/2)(B_0' - 3)(1-x) + (\varsigma - (3/2))(1-x)^2], \tag{13}$$

where

$$x = (V/V_0)^{1/3} \qquad \text{and} \qquad \varsigma = (3/8)(B_0' - 1)(B_0' + 3) + (3/2)B_0 B_0'' + (1/3).$$

Poirier and Tarantola [35] questioned the fundamental bases of both Love and Birch approaches, and strongly asserted that the Hencky strain formalism is the correct one. Accordingly, they proposed an EOS explicit up to the two-parameter level only. The three-parameter extension of this EOS, which was recently tested by Stacey and Davis [41] against the geophysical data, and Sushil *et al* [39] against theoretical data, may be expressed as

$$P = (V_0/V)B_0[\ln(V_0/V) + (1/2)(B_0' - 2)(\ln(V_0/V))^2 + (1/6)(B_0 B_0'' + B_0'^2 - 3B_0' + 3)(\ln(V_0/V))^3]. \tag{14}$$

Very recently Sushil *et al* [39], following the path of Birch but using $n = 1$ instead of $n = 2$ in the Eulerian strain measure $f = (1/n)[(V/V_0)^{-n/3} - 1]$, and using the method of Stacey [78], proposed a modified three-parameter Eulerian strain EOS,

$$P = (9/2)B_0[-A_1 x^{-4/3} + A_2 x^{-5/3} - A_3 x^{-2} + A_4 x^{-7/3}], \tag{15}$$

where

$$x = (V/V_0), \qquad A_1 = B_0 B_0'' + (B_0' - 3)^2 + (26/9),$$
$$A_2 = 3B_0 B_0'' + (B_0' - 3)(3B_0' - 8) + (66/9),$$
$$A_3 = 3B_0 B_0'' + (B_0' - 3)(3B_0' - 7) + (60/9)$$
$$\text{and} \qquad A_4 = B_0 B_0'' + (B_0' - 3)(B_0' - 2) + (20/9).$$

Further, Sushil *et al* claimed that their EOS based on a modified Eulerian strain is more rapidly convergent than the Birch–Murnaghan EOS founded on the Eulerian strain.

Bose Roy and Bose Roy [36] suggested a three-parameter EOS in the realistic form

$$V/V_0 = 1 - \{(\ln(1 + aP))/(b + cP)\}. \tag{16}$$

Here,

$$a = (1/8B_0)[3(B_0' + 1) + (25B_0'^2 + 18B_0' - 32B_0 B_0'' - 7)^{1/2}],$$
$$b = (1/8)[3(B_0' + 1) + (25B_0'^2 + 18B_0' - 32B_0 B_0'' - 7)^{1/2}]$$

and

$$c = [(1/16)[3(B_0' + 1) + (25B_0'^2 + 18B_0' - 32B_0 B_0'' - 7)^{1/2}]] \times [(B_0' + 1) - (1/8)[3(B_0' + 1) + (25B_0'^2 + 18B_0' - 32B_0 B_0'' - 7)^{1/2}]].$$

We mention below some EOSs which have often been applied/discussed in the literature, although their behaviour towards experiment, at high pressures, is at wide variance with the EOSs referred to above.

Following Bridgman's approach [16], Taylor expansion of V in powers of P around $P = 0$, to third degree, the EOS obtained is

$$V/V_0 = 1 - (1/B_0)P + (1/2)(1/B_0^2)(B_0' + 1)P^2 - (1/12)(1/B_0^3)(4B_0'^2 + 6B_0' - 2B_0 B_0'' + 2)P^3. \tag{17}$$

Slater's [12] expansion of pressure as polynomial in volume compression, $(1 - V/V_0)$, up to the cubic term yields

$$P = B_0(1 - V/V_0) + (1/2)B_0(B_0' + 1)(1 - V/V_0)^2 + (1/12)B_0(2B_0'^2 + 6B_0' + B_0B_0'' + 4)(1 - V/V_0)^3. \quad (18)$$

An alternative approach has been suggested by Onat and Vaisnys [15], whereby the pressure is expanded in powers of $\ln V$ about $V = V_0$, giving

$$P = -B_0 \ln(V/V_0) + (1/2)B_0B_0'[\ln(V/V_0)]^2 - (1/6)(B_0^2B_0'' - B_0B_0'^2)[\ln(V/V_0)]^3. \quad (19)$$

Cubic inverse volume EOS, as discussed by Macdonald [80], is

$$V/V_0 = [1 + (1/B_0)P - (1/2)(1/B_0^2)(B_0' - 1)P^2 + (1/12)(1/B_0^3)(4B_0'^2 - 6B_0' - B_0B_0'' + 2)P^3]^{-1}. \quad (20)$$

A two-parameter Lagrangian EOS is documented in Murnaghan's 1951 monograph [5]. It will be interesting to study the three-parameter extension of this EOS [17] from an application point of view. With $n = -2$, in the Lagrangian strain measure, $f = (1/n)[(V/V_0)^{-n/3} - 1]$, the EOS obtained, in line with Stacey [78], is

$$P = (9/16)B_0[\{(B_0B_0'' + 3B_0' + B_0'^2 + (23/9))(V/V_0)^{-1/3}\} - \{(3B_0B_0'' + 7B_0' + 3B_0'^2 + (7/3))(V/V_0)^{1/3}\} + \{(3B_0B_0'' + 5B_0' + 3B_0'^2 - (1/3))(V/V_0)\} - \{(B_0B_0'' + B_0' + B_0'^2 - (1/9))(V/V_0)^{5/3}\}]. \quad (21)$$

3. Application to model-independent experimental isotherms: results and discussions

All the 21 EOSs presented in section 2 are fitted to the EOS data of nine solids, differing considerably in their bulk modulus values, namely Ag, Al, Mg, Pd, MgO [56], NaCl [57], Cu [58], Mo and W [59]—corresponding to the regression curves of P on V/V_0. These data are not directly measured isotherms, but are computed reductions of shock Hugoniot data to isotherms. However, these data are accurate enough to allow a meaningful discrimination between the applicabilities of the EOS models. Moreover, these data are also model independent as they are not biased by any of the isothermal EOSs considered in the present study. The original isotherms of the above solids, referred to hereafter as the high-pressure isotherms, are abbreviated as HPIs. The subsets of these HPIs, from the pressure values $P = 0$ to a low pressure maximum, referred to hereafter as low-pressure isotherms, are abbreviated as LPIs. The details related to these HPIs and LPIs are summarized in table 1. The experimental bulk modulus values, chosen for the purpose of comparison with the fit parameters for HPIs, are tabulated in table 2. The root-mean-square deviations (RMSDs) between the data points (HPIs) and fits are reported in table 3. The values of the fit bulk modulus parameters, as such, are not shown. Instead, the deviation parameters, D_i ($i = 1, 2, 3, 4, 5$), which are more important and meaningful for comparing the applicability of the EOSs, are computed and compared in tables 4–8. D_1 values refer to the percentage deviations of the fit values of B_0 inferred from the HPIs from those of the fit values of B_0 inferred from the LPIs, for all the isotherms of the solids considered. Moreover, likewise, D_2 values and D_3 values refer to the corresponding deviations of B_0' and B_0'', respectively, while D_4 values and D_5 values are the percentage deviations of the fitted B_0 and B_0' from the corresponding experimental values. It may be noted that the EOSs are arranged in decreasing order of their relative performance as

Table 1. Details related to the isotherms of solids and their subsets used in the study. n denotes the number of data points.

			High-pressure isotherm (HPI)			Low-pressure isotherm (LPI)		
Solids	References	T (K)	n	P_{max} (kbar)	MRV	n	P_{max} (kbar)	MRV
Ag	[56]	293	57	1 500	0.6519	29	145	0.9017
Al	[56]	293	49	1 100	0.6083	20	100	0.9010
Cu	[58]	300	10	10 040	0.436	8	5420	0.502
Mg	[56]	293	41	700	0.5510	8	40	0.9081
Mo	[59]	293	30	3 000	0.6305	8	800	0.8167
Pd	[56]	293	67	2 000	0.6831	32	250	0.9018
W	[59]	293	30	3 000	0.6552	8	800	0.8347
MgO	[56]	293	51	850	0.7046	31	200	0.9017
NaCl	[57]	293	40	200	0.7023	8	40	0.8849

Table 2. Experimental values of B_0 and B_0' used for comparison purposes.

Solids	B_0 (Expt) (kbar)	References	B_0' (Expt)	References
Ag	1047[a]	[61, 62]	5.53	[63]
Al	742 ± 8	[64]	4.72	[65]
Cu	1420	[61]	5.25	[66]
Mg	344.20	[67]	4.16	[67]
Mo	2653	[61]	4.5 ± 0.5	[68]
Pd	1808	[62]	5.3 ± 0.2	[68]
W	3084	[69]	4.0 ± 0.2	[68]
MgO	1560	[71]	4.52	[72]
NaCl	238.35	[49]	5.11	[48]

[a] An average of the two values.

we move down tables 3–8. It may be noted that RMSDs in table 3, and D_i values in tables 4–8 are arranged in such a way that the number of solids for which these values are of lower magnitude is higher in any row than the rows that follow down the table. Further, it may be noted that results are shown for 16 EOSs only, because we observe that the performance of equations (17)–(21) is very poor, and does not merit any consideration for comparison, on a relative scale, along with the rest of the EOSs. However, we have noted our observations on the performance of these models in the later sections.

3.1. Fitting accuracy

Fitting accuracy is assessed, in terms of root-mean-square deviations (RMSDs) between the data points and fits. Fitting accuracy is a measure of the agreement between the data points and fits, and not a measure, it must be emphasized, of the agreement between the data curves and fit curves. Though, in general, a good curve-fitting capability is observed for an EOS that exhibits a good fitting accuracy, this is not always true [37, 55]. This coincidence often prompted the workers in the past to investigate the applicability of an EOS on the basis of fitting accuracy alone, and unfortunately, this trend still continues [44]. An EOS that describes the data points very successfully but fails to describe the data curves is of no utility from an application point of view, even for interpolation purposes [55].

Table 3. Root-mean-square deviations (RMSDs) between the data points and fits corresponding to the regression curves of P on V/V_0 (in kbar) for selected solids.

	3-parameter EOS	Ag	Al	Cu	Mg	Mo	Pd	W	MgO	NaCl
1	Bose Roy–Bose Roy	0.18	0.21	17.80	0.19	1.03	0.24	0.41	0.24	0.078
2	Birch–Murnaghan	0.809	0.433	25.56	0.27	1.247	0.72	0.66	0.263	0.085
3	Keane	0.807	0.40	30.00	0.34	1.250	0.71	0.61	0.264	0.12
4	Mie–Gruneisen	0.813	0.447	35.82	0.345	1.295	0.7287	0.686	0.270	0.45
5	Holzapfel	0.80	0.450	27.75	0.347	1.300	0.7286	0.689	0.272	0.091
6	Hama–Suito	0.88	0.47	30.83	0.385	1.32	0.80	0.71	0.281	0.0949
7	SASS	1.10	0.46	36.62	0.36	1.298	0.981	0.688	0.284	0.0999
8	Davis–Gordon	1.17	0.428	39.62	0.37	1.27	1.04	0.64	0.283	0.1099
9	Universal	0.91	0.49	31.20	0.40	1.35	0.82	0.74	0.285	0.0941
10	Mao	0.886	0.54	22.28	0.389	1.41	0.84	0.83	0.299	0.0951
11	Freund–Ingalls	0.888	0.56	23.02	0.392	1.44	0.85	0.88	0.304	0.081
12	Huang–Chow	0.903	0.60	21.05	0.41	1.48	0.87	0.94	0.31	0.083
13	Kumari–Dass	0.959	0.73	17.91	0.442	1.65	0.97	1.16	0.359	0.080
14	Murnaghan	0.961	0.75	18.40	0.444	1.67	0.98	1.20	0.365	0.090
15	Luban	0.97	0.77	16.70	0.45	1.75	0.99	1.23	0.38	0.102
16	Poirier–Tarantola	1.70	0.60	55.06	0.58	1.46	1.55	0.84	0.37	0.1100

Table 4. Percentage deviations in the fit values of B_0 for the HPI from those of B_0 for the LPI, denoted by D_1 in the text.

	3-parameter EOS	Ag	Al	Cu	Mg	Mo	Pd	W	MgO	NaCl
1	Bose Roy–Bose Roy	0.47	1.28	5.22	0.95	0.26	0.33	0.42	0.20	−0.29
2	Mie–Gruneisen	2.273	3.49	44.50	2.70	1.05	1.42	0.55	0.2613	0.38
3	Keane	2.275	1.93	27.71	3.28	1.09	1.37	0.84	0.2614	−3.05
4	Birch–Murnaghan	2.37	2.18	16.79	2.69	1.16	1.421	1.00	0.2614	−1.34
5	Holzapfel	2.37	2.20	26.21	3.49	1.31	1.42	1.03	0.33	−1.71
6	Hama–Suito	2.654	2.28	33.37	3.91	1.39	1.58	1.10	0.391	−1.88
7	Universal	2.654	2.36	33.83	4.054	1.46	1.69	1.16	0.391	1.88
8	SASS	3.32	2.23	−34.09	3.61	1.28	1.97	1.03	0.392	−2.26
9	Davis–Gordon	3.60	2.06	42.84	3.61	1.16	2.08	0.94	0.392	−2.76
10	Mao	2.652	2.77	12.66	3.99	1.65	1.80	1.3889	0.46	−1.80
11	Freund–Ingalls	2.75	2.82	13.63	4.053	1.72	1.80	1.49	0.52	−0.79
12	Huang–Chow	2.75	3.02	10.51	4.20	1.87	1.91	1.61	0.59	−1.00
13	Luban	3.03	2.89	4.61	3.70	2.32	2.18	2.03	0.78	−0.41
14	Kumari–Dass	3.13	3.53	5.47	4.55	2.28	2.24	1.97	0.78	0.63
15	Murnaghan	3.13	3.57	6.13	4.58	2.32	2.24	2.03	0.72	1.21
16	Poirier–Tarantola	5.78	2.97	63.36	6.01	1.84	3.44	1.39	0.85	−2.72

Table 3 shows that the RMSDs inferred from our model (equation (16)) are lower than those inferred from the rest of the EOSs by a variable factor, rising to as high as 4. The solitary exception is the one yielded by the Luban EOS (equation (8)) for the isotherm of Cu only. All the EOSs, in sharp contrast with the excellent performance of equation (16), utterly fail to describe the data curve for Cu. That even the Luban EOS as discussed in the next section, with a fitting accuracy slightly better than ours, proves no exception endorses the dictum that the fitting accuracy alone cannot certify the validity of an EOS.

3.2. Fit parameters: stability and agreement with experiment

The assumption of constant variance of random disturbance distribution, and the assumption that the systematic biases are weak or absent for an accurate experimental isotherm,

Table 5. Percentage deviations in the fit values of B_0' for the HPI from those of B_0' for the LPI, denoted by D_2 in the text.

	3-parameter EOS	Ag	Al	Cu	Mg	Mo	Pd	W	MgO	NaCl
1	Bose Roy–Bose Roy	−2.81	−10.15	3.74	−6.46	−1.45	−1.63	−2.63	0.58	1.85
2	Mie–Gruneisen	−10.04	−15.39	−89.57	−10.88	−3.77	−6.49	−2.10	−2.18	−3.58
3	Birch–Murnaghan	−10.16	−14.6	−23.13	16.0	−4.77	−6.34	−5.21	−2.37	7.08
4	Keane	−10.37	−14.7	−45.60	−19.02	−5.17	−6.20	−4.93	−2.65	17.60
5	Holzapfel	−10.52	−15.26	−48.36	−19.48	−6.04	−6.59	−5.85	−2.96	8.84
6	Luban	−11.14	−12.99	−5.84	−9.63	−9.58	−8.94	−9.59	−4.96	5.62
7	SASS	−15.78	−15.64	−55.23	−19.90	−5.99	−10.09	−5.87	−3.75	12.45
8	Hama–Suito	−12.01	−15.88	−67.61	−21.28	−6.62	−7.67	−6.21	−3.67	10.0
9	Davis–Gordon	−17.54	−15.11	−74.04	−20.31	−5.61	−11.16	−5.36	−3.90	15.72
10	Universal	−12.3	−16.4	−69.79	−22.1	−7.1	−7.9	−6.59	−3.89	9.77
11	Freund–Ingalls	−11.69	−17.88	−19.94	−21.05	−7.90	−8.19	−7.75	−4.27	3.82
12	Mao	−11.79	−18.72	−19.16	−21.30	−7.84	−8.18	−7.63	−4.34	9.60
13	Huang–Chow	−11.93	−19.23	−14.66	−21.60	−8.50	−8.49	−8.35	−4.60	4.97
14	Murnaghan	−12.17	−19.38	−7.82	−21.85	−9.36	−9.36	−9.42	−5.39	−4.86
15	Kumari–Dass	−12.28	−19.95	−6.85	−22.02	−9.41	−9.35	−9.41	−5.51	−2.84
16	Poirier–Tarantola	−29.65	−20.38	−166.7	−30.52	−9.40	−19.93	−8.32	−7.92	15.86

Table 6. Percentage deviations in the fit values of $B_0''/n/B_\alpha'$ for the HPI from those of $B_0''/n/B_\alpha'$ for the LPI, denoted by D_3 in the text. B_0'', n and B_α' are treated as free parameters.

	3-parameter EOS	Ag	Al	Cu	Mg	Mo	Pd	W	MgO	NaCl
1	Bose Roy–Bose Roy	−18.9	−61.8	−9.25	−54.1	−8.77	−4.94	−17.7	−0.44	6.44
2	Keane	55.2	250	23.1	196.1	10.4	5.41	14.2	13.0	−32.1
3	Mie–Gruneisen	−76.3	−39.2	−1779	−65.3	−23.2	−55.0	−12.1	−35.4	−21.2
4	Birch–Murnaghan	−73.9	−75.5	−85.0	−79.6	−30.2	−51.5	−35.7	−36.2	46.1
5	SASS	−130.5	−79.7	242.6	−91.6	−43.3	−111.1	−43.9	−56.0	95.2
6	Davis–Gordon	−151.4	−77.9	127.5	−93.3	−41.3	−132.5	−40.8	−58.8	127.2
7	Hama–Suito	−95.3	80.6	584.1	−96.7	−49.8	−73.7	−47.5	−55.1	68.0
8	Universal	−98.4	−82.3	409.3	−99.2	−54.5	−77.2	−50.9	−58.0	66.7
9	Freund–Ingalls	−90.4	−88.0	−5025	−95.8	−61.2	−76.7	−60.4	−62.8	18.58
10	Mao	−90.7	−89.3	−4282	−96.1	−61.1	−76.6	−60.0	−63.5	74.0
11	Huang–Chow	−92.3	−91.3	9302	−97.1	−67.2	−80.4	−66.0	−67.2	30.0
12	Luban	−95.53	−86.56	438.7	−105.6	−77.89	−88.58	−76.72	−68.15	818.4
13	Murnaghan	−96.4	−94.5	1125	−98.5	−77.1	−89.9	−76.1	−77.9	−44.5
14	Kumari–Dass	−96.1	94.9	−93.6	−98.61	−98.6	−74.8	−88.9	−73.6	−77.3
15	Poirier–Tarantola	−308.8	−96.7	−56.5	−123.7	−79.8	−340.0	−68.6	−119.9	145.9
16	Holzapfel	188.7	134	90.6	−159.4	146.8	52.8	212.2	107.4	−1303

implies that when an adequate (i.e., a true hypothetical) EOS model is fitted to the various pressure/compression ranges of an isotherm, the same set of fit bulk moduli parameters should be obtained. In practice, however, a disagreement is observed between different sets of fit parameters, when an EOS is applied to various pressure/compression ranges of an isotherm. The observed disagreement may be attributed to the inadequacy of the real EOS model, and to the real data which are data of limited span and precision. However, for the various ranges of the same set of compression data, the magnitude of such disagreements in the fit parameters, observed for various EOS models, may well serve as a test to assess the adequacies of the considered EOSs, on a relative scale.

Table 7. Percentage deviations in the fit values of B_0 for the HPI from those of B_0 from experiment, denoted by D_4 in the text. Deviations related to the LPI of Cu included.

	3-parameter EOS	Ag	Al	Cu (HPI)	Cu (LPI)	Mg	Mo	Pd	W	MgO	NaCl
1	Bose Roy–Bose Roy	1.34	3.60	−1.48	(2.61)	−1.48	0.79	1.60	0.84	−1.99	0.15
2	Keane	3.06	4.03	46.06	(14.37)	1.39	1.51	2.60	1.17	−1.67	−2.79
3	Birch–Murnaghan	3.15	4.39	31.76	(12.75)	0.81	1.66	2.65	1.39	−1.67	−1.03
4	Mie–Gruneisen	3.15	4.37	65.56	(14.58)	1.54	1.73	2.71	1.39	−1.60	0.99
5	Holzapfel	3.15	4.38	44.79	(14.72)	1.60	1.77	2.71	1.39	−1.60	−1.41
6	Hama–Suito	3.44	4.46	55.63	(16.69)	2.00	1.85	2.88	1.46	−1.54	−1.62
7	Universal	3.44	4.53	57.11	(17.32)	2.15	1.92	2.93	1.52	−1.54	−1.57
8	Mao	3.53	4.91	30.99	(17.32)	2.12	2.19	3.10	1.78	−1.41	−1.49
9	Freund–Ingalls	3.63	5.05	32.11	(18.03)	2.18	2.30	3.10	1.91	−1.41	−0.44
10	Huang–Chow	3.63	5.20	28.87	(16.27)	2.32	2.45	3.21	2.04	−1.35	−0.65
11	SASS	4.11	4.39	−57.32	(16.27)	1.71	1.73	3.26	1.39	−1.54	−1.99
12	Davis–Gordon	4.39	4.20	68.59	(16.62)	1.71	1.62	3.37	1.26	−1.54	−2.50
13	Kumari–Dass	4.01	5.82	23.59	(17.18)	2.70	2.94	3.54	2.50	−1.15	1.03
14	Luban	4.01	5.89	23.17	(17.18)	2.73	2.98	3.54	2.53	−1.15	0.78
15	Murnaghan	4.01	5.93	24.37	(34.72)	2.73	3.02	3.54	2.59	−1.15	1.62
16	Poirier–Tarantola	6.59	5.12	120.1	(17.75)	4.07	2.30	4.76	1.75	−1.09	−2.41

Table 8. Percentage deviations in the fit values of B_0' for the HPI from those of B_0' from experiment, denoted by D_5 in the text. Deviations related to the LPI of Cu included.

	3-parameter EOS	Ag	Al	Cu (HPI)	(Cu) (LPI)	Mg	Mo	Pd	W	MgO	NaCl
1	Bose Roy–Bose Roy	4.3	9.5	−2.9	(−6.4)	0.5	3.0	0.9	1.8	0.4	2.47
2	Keane	−10.94	−10.68	−59.58	(−25.69)	−10.63	−5.6	−5.26	−2.7	−2.35	20.82
3	Birch–Murnaghan	11.0	12.3	−39.6	(−21.45)	7.9	6.3	5.5	4.0	2.4	9.47
4	Mie–Gruneisen	−11.19	−12.39	−92.28	(−25.96)	−11.15	−6.93	−5.68	−4.2	−2.83	−4.15
5	Holzapfel	−11.28	−12.46	−61.89	(−26.19)	−11.47	−7.05	5.792	−4.23	−2.96	11.35
6	SASS	−16.49	−12.56	−69.20	(−31.2)	−11.85	−6.98	−9.42	−4.23	−3.56	15.21
7	Hama–Suito	−12.78	−12.92	−77.50	(−30.55)	−13.37	−7.55	−6.91	−4.53	−3.50	12.58
8	Davis–Gordon	−18.23	−11.67	−82.75	(−33.56)	−12.12	−6.28	−10.49	−3.38	−3.58	18.69
9	Universal	13.0	13.3	−79.4	(−31.9)	14.2	8.0	7.2	5.0	3.8	12.33
10	Mao	−12.89	−15.11	−41.35	(−28.34)	−13.56	−9.43	−7.62	−6.53	−4.45	11.68
11	Freund–Ingalls	−12.95	−15.74	−42.63	(−28.34)	−13.70	−9.95	−7.74	−7.18	−4.67	5.38
12	Huang–Chow	−13.22	−16.42	−39.10	(−28.65)	−14.23	−10.65	−8.06	−7.83	−5.00	6.58
13	Kumari–Dass	−14.09	−18.75	−33.94	(−29.09)	−15.36	−12.63	−9.26	−10.0	−6.33	−2.29
14	Luban	−14.16	−18.81	−33.62	(−29.50)	−15.43	−12.70	−9.34	−10.00	−6.35	−1.12
15	Murnaghan	−14.10	−19.03	−34.63	(−29.09)	−15.41	−12.88	−9.34	−10.3	−6.46	−4.54
16	Poirier–Tarantola	−30.54	−16.89	−123.4	(−65.01)	−23.34	−10.38	−19.64	−6.6	−7.70	18.38

A high degree of ambiguity accompanies the measured bulk moduli data even for a substance as simple as NaCl [37], and also as stable as Cu. However, the problem of selection of experimental bulk modulus data, for the purpose of comparison with the fit parameters, is resolved in line with our earlier approach [37]. We have observed a spectacular convergence of equations (1)–(16) for the LPIs—except for the LPI of Cu for which the pressure ranges to well above 5 Mbar and the maximum compression suffered is about 50%—which accords well with some of the earlier observations [37, 51–53]. Further, we have observed that even the equations (17)–(21), whose curve-fitting capability at high pressure is very poor, also tend

to converge for the LPIs. In particular, the EOS proposed by Onat and Vaisnys (equation (19)) is on a par with equations (1)–(16) for the LPIs. Because in the low-pressure region the fit parameters are virtually independent of the analytical forms of the EOS models chosen, these values may be considered as the closest approximation to the real bulk modulus values of the solids. Therefore the bulk modulus data, which are closest to the values to which the considered EOSs converge, are selected in table 2 for the comparison purposes—and therefore the selection of data is not arbitrary. Notably, even for Cu, which is predicted to remain stable in the fcc structure up to at least 2.5 TPa [58], there is a considerable disagreement among the three sets of literature values of B_0, 1370 [62], 1420 [61], and 1332 ± 20 kbar [68], while the values of B_0', 5.4(±2) [68] and 5.25 [61], agree well. The rationale for choosing the value of 1420 kbar for Cu (table 2) for comparison is that, for the LPI of Cu, all the EOSs yield fit values of B_0 which are higher than this value.

Table 4 shows that D_1 values inferred from our model (equation (16)) are significantly lower than those from the rest of the EOSs—the only exception is the one from the Luban EOS for Cu, proving lower than ours. A similar relative performance of the EOSs is noted for the D_2 test, in table 5. The Mie–Gruneisen EOS is the only one that proves more stable than ours, for W. Turning to D_3 (table 6), although all the EOSs are, in general, very large compared to ours, there are two points, those of Al and W from the Mie–Gruneisen EOS, for which the registered D_3 values are lower than equation (16).

D_4 (table 7) reflects the goodness of the agreement of the fit parameter B_0 with experiment. Here, equation (16) agrees with experiment within 2%, with the exception of Al disagreeing to 3.6% only. However, the agreement shown by the Keane and Birch–Murnaghan EOSs for Mg, and the Poirier and Tarantola EOSs for MgO, is better than shown by our equation.

Focusing on D_5 (table 8), it can be noticed that for equation (16) the agreement of the fit B_0' with experiment is quite remarkable. Equation (16) mimics the experiment well within 1% for as many as three solids. The mismatch with four others does not exceed 3%, but for Ag it exceeds 4%, while the highest disagreement is observed for Al, but still the mismatch remains well within 10%. It is only the Kumari and Dass equation that agrees slightly better than ours for NaCl.

It must be noted that in assessing the relative performances we have given equal weight to the numerical values related to the D_i values. A question of considerable importance is whether the 10% deviations in the fit values of B_0 have the same bearing on the adequacy of the EOSs as the 10% deviations in the fit values of B_0'—of course not. Obviously, the EOSs may be arranged in tables 4–8, using different points of justification regarding the weight to be attached to the D_i values, and thus the trends depicted for the relative utility may vary slightly. Further, the position of relative utility may also vary by imposing an upper limit of validity to the test-points. But what will not vary is the relative utility of our model—irrespective of the methodology adopted for the purposes—with a well pronounced difference from all the EOSs compared.

Furthermore, we must emphasize that small values of D_1 and D_2 may be misconstrued as positive attributes to the adequacy of an EOS, unless the corresponding D_4 values and D_5 values are also small. To illustrate the point, we refer to tables 4 and 5, where the small values of D_1(4.61%) and D_2 (−5.84%) for Cu might seem to lend credence to the adequacy of the Luban EOS. But this is belied on a close examination of tables 7 and 8. Here, it can be seen that the fit values of B_0 from both the HPIs and LPIs are considerably higher than the experiment, but their mutual difference is not that large, leading to a small D_1 in table 4. Likewise, although both the fit values of B_0' are considerably lower than the experiment, they are mutually not far apart, resulting in a misleading small value for D_2. The position with the Kumari and Dass and the Murnaghan equations is similar.

Table 9. Number of wiggles of the data deviation curves about the fits (NW).

	3-parameter EOS	Ag	Al	Cu	Mg	Mo	Pd	W	MgO	NaCl
1	Bose Roy–Bose Roy	15	11	4	13	12	17	11	24	17
2	Birch–Murnaghan	3	5	3	7	7	5	5	21	16
3	Keane	3	7	3	5	7	5	7	21	11
4	Holzapfel	3	5	3	5	7	5	5	21	14
5	Mie–Gruneisen	3	5	3	5	8	5	5	21	2
6	Hama–Suito	3	5	3	3	7	5	5	21	14
7	SASS	3	5	3	5	7	5	5	19	11
8	Davis–Gordon	3	5	3	3	7	3	7	19	11
9	Universal	3	5	3	3	5	5	5	19	14
10	Kumari–Dass	5	3	3	5	5	5	3	15	17
11	Huang–Chow	3	3	3	5	5	5	3	19	16
12	Luban	5	3	3	5	5	5	3	11	15
13	Freund–Ingalls	3	3	3	5	5	5	3	19	14
14	Mao	3	3	3	5	5	5	3	17	13
15	Murnaghan-3	5	3	3	5	5	5	3	11	11
16	Poirier–Tarantola	3	5	3	3	5	3	3	15	11

3.3. Departure of the data deviation plot from the normal error curve and adequacy of EOS

As already mentioned, measured isothermal compression data are biased by both the systematic and random disturbances. If the systematic error is insignificant, and random errors are small, a reasonable assumption for an isotherm claimed as accurate, the randomization of the data points about the regression curve—when a hypothetical true EOS model, adequate within the ranges of the data, is fitted to these isotherms—may be best approximated by the normal error curve. The data points are evenly randomized about this true (hypothetical) regression curve. Because of the indeterminate nature of the random error, we cannot however draw the true regression curve. In practice, due to the inadequacy of the EOS model considered, systematic biases come into play, and the cumulative effect of the systematic slant on the random biases forces the data distribution to depart from the normal random variable distribution pattern. An appreciation of the inadequacy of the considered EOSs is possible by an enumeration of the wiggles of the data deviation curves about the fits—each turn indicating the distribution of the positive and negative deviations around the regression curve. Obviously the number of wiggles of the data deviation curve (referred to as NW in tables 9 and 10) about the true regression curve would be a maximum for the hypothetical true EOS model, and would decrease with decreasing closeness of a real EOS with the true EOS model. It can be argued therefore that the curve-fitting capability of the EOSs can be compared on the basis of the departure of the data deviation curves from the ideal normal random variable curve. If two EOSs differ significantly from each other with regard to their curve-fitting capability, it would be manifest in the significant difference in the number of wiggles of their data deviation curves. If, however, the difference from each other is not very significant, or marginal, the same may be reflected in the marginal difference in the number of wiggles, or merely in the degree of departures of their data deviation curves from the symmetric normal random distribution pattern, and an explicit difference in the number of wiggles may not be registered. In order to assess any significant difference in the fitting capability of the EOSs compared, we have plotted the deviation in the response, P, against the regressor, V/V_0, inferred from all the EOSs for all the nine isotherms considered, and counted the number of times the data deviation curves cross the fit. The enumerated numerical values are tabulated in table 9. It may be noted that the

Table 10. Overall relative performance of the EOSs based on their relative performances against the seven tests as shown in tables 3–9.

	3-parameter EOS	RMSD	D_1	D_2	D_3	D_4	D_5	NW
1	Bose Roy–Bose Roy	1	1	1	1	1	1	1
2	Keane	3	3	4	2	2	2	3
3	Birch–Murnaghan	2	4	3	4	3	3	2
4	Mie–Gruneisen	4	2	2	3	4	4	5
5	Holzapfel	5	5	5	15	5	5	4
6	SASS	6	6	7	7	6	7	6
7	Hama–Suito	7	8	6	5	11	6	7
8	Davis–Gordon	8	9	8	6	12	8	8
9	Universal	9	7	9	8	7	9	9
10	Mao	10	10	11	10	8	10	13
11	Freund–Ingalls	11	11	10	9	9	11	12
12	Huang–Chow	12	12	12	11	10	12	11
13	Kumari–Dass	13	13	14	13	13	13	10
14	Luban	15	13	6	12	14	14	12
15	Murnaghan	14	14	13	12	14	14	14
16	Poirier–Tarantola	15	15	15	14	15	15	15

numerical values of NW are so arranged that, on an overall basis, in any row the number of isotherms for which a higher number of wiggles is inferred from an EOS is higher than those that follow down the table.

Table 9 shows that for Ag, Al, Mg, Mo, Pd, and W there is a significant difference between the number of wiggles (NW) inferred from our EOS and the rest of the 15 EOSs compared, thus indicating that, on a relative scale, equation (16) is much closer to the true EOS model, compared to others. Notably, the number of wiggles is also higher for the NaCl and MgO isotherms where the maximum compression ranges are relatively small. It is also remarkable that even for the Cu isotherm, comprising only ten data points, equation (16) yields a higher number of wiggles. Further, it may be noted that the difference in the number of wiggles, between the rest of the successive EOSs down the table, is not that wide.

3.4. Overall position of relative utility

The overall position of the EOSs, with regard to their relative utility, is depicted in table 10. In this table, the relative performance of the individual EOSs against the seven tests—the fitting accuracy; stability of the fit parameters B_0, B_0', and B_0''; agreement of the fit parameters B_0 and B_0' with experiment; and randomization of the data points about the fits (NW)—is expressed in terms of the numerical values denoting their relative positions with reference to their individual responses to the said tests in tables 3–9. It must be emphasized that these numerical values do not constitute any quantitative scale. They simply indicate that the higher the numerical value, the lower the rating against the tests specified at the column heads, on a relative scale. It can be seen (tables 3–10) that our model is, in general, far superior to the nearest rivals, the Keane and Birch–Murnaghan equations, on all seven tests—but the difference between the successive EOSs, down the tables, is not so large. It must be emphasized here that all seven tests are highly correlated, and none of them is singularly sufficient to assess the adequacy of an EOS. In figures 1(a)–6(b), we compare and examine the deviations between the data points and data fits with various equations. All the EOSs are systematically high at low and high pressures. One important feature, which is conspicuous in all the graphs, is that the fits

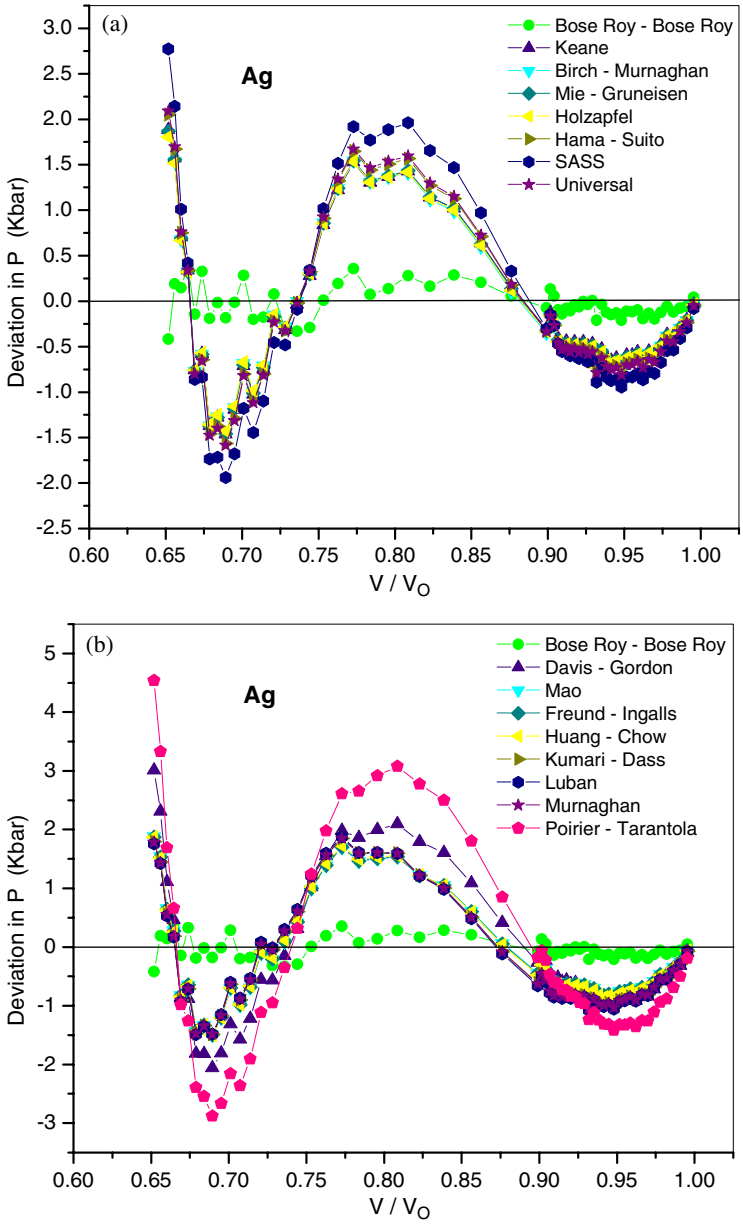

Figure 1. (a) and (b). Comparison of deviations between the data curve of Ag [56] and the fits from Bose Roy–Bose Roy, and the other equations of state.

yielded by equation (16), result in a very accurate representation of the data. The magnitude of systematic deviations at low pressure is appreciably low—a characteristic of a well behaved EOS that helps in the extraction of accurate values of fit parameters [22], and is much lower than those arising from all the other EOSs. Moreover, randomization of the data points about the fits is also decisively better—the deviation curves hovering closely around the fits, over the entire pressure ranges, while the deviation points yielded by the other EOSs huddle together,

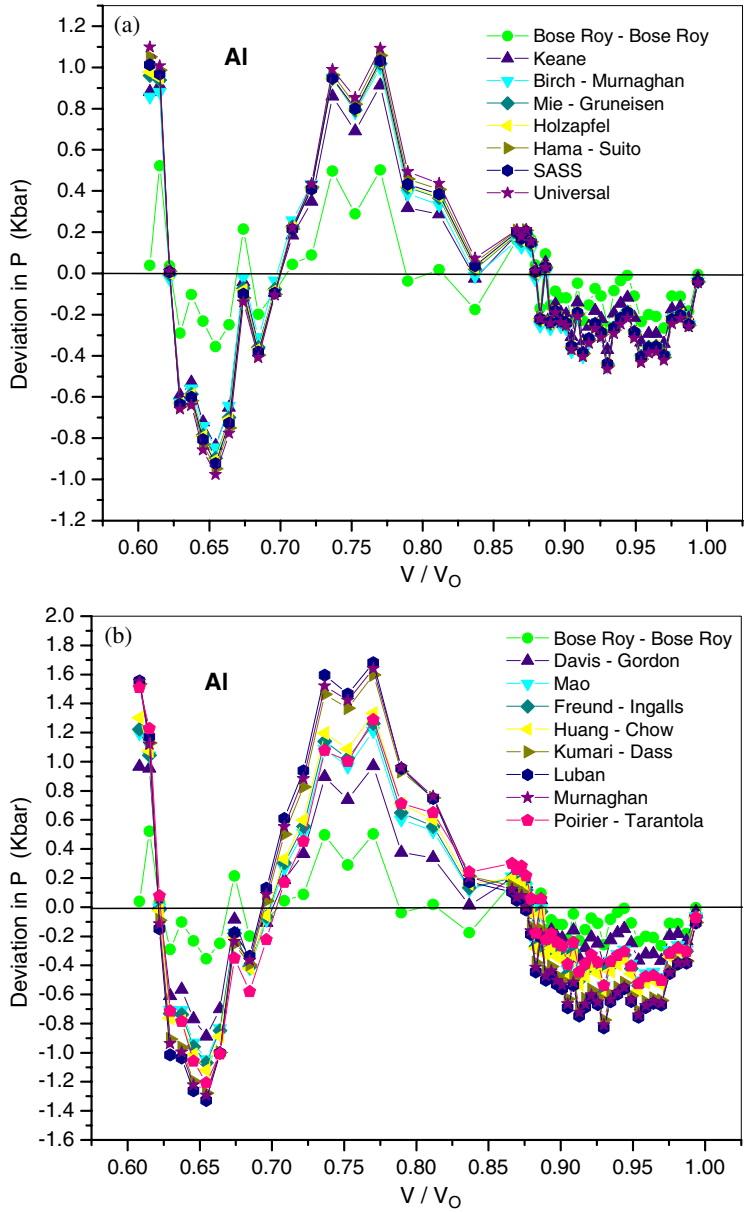

Figure 2. (a) and (b). Comparison of deviations between the data curve of Al [56] and the fits from Bose Roy–Bose Roy, and the other equations of state.

especially at low and high pressures, indicating that the difference in the curve-fitting capability of these EOSs is not as pronounced as the difference between them and equation (16).

Our observation that there is no significant difference in the curve-fitting capability between the Birch–Murnaghan and Keane EOSs (tables 3–10), based on the real experimental compression data, accords well with the Macdonald and Powell conclusion [51]—based on the use of exact synthetic data over smaller pressure ranges—that the actual discrimination between these EOSs is nugatory. Anderson [16] has used a variety of shock-wave measurements on

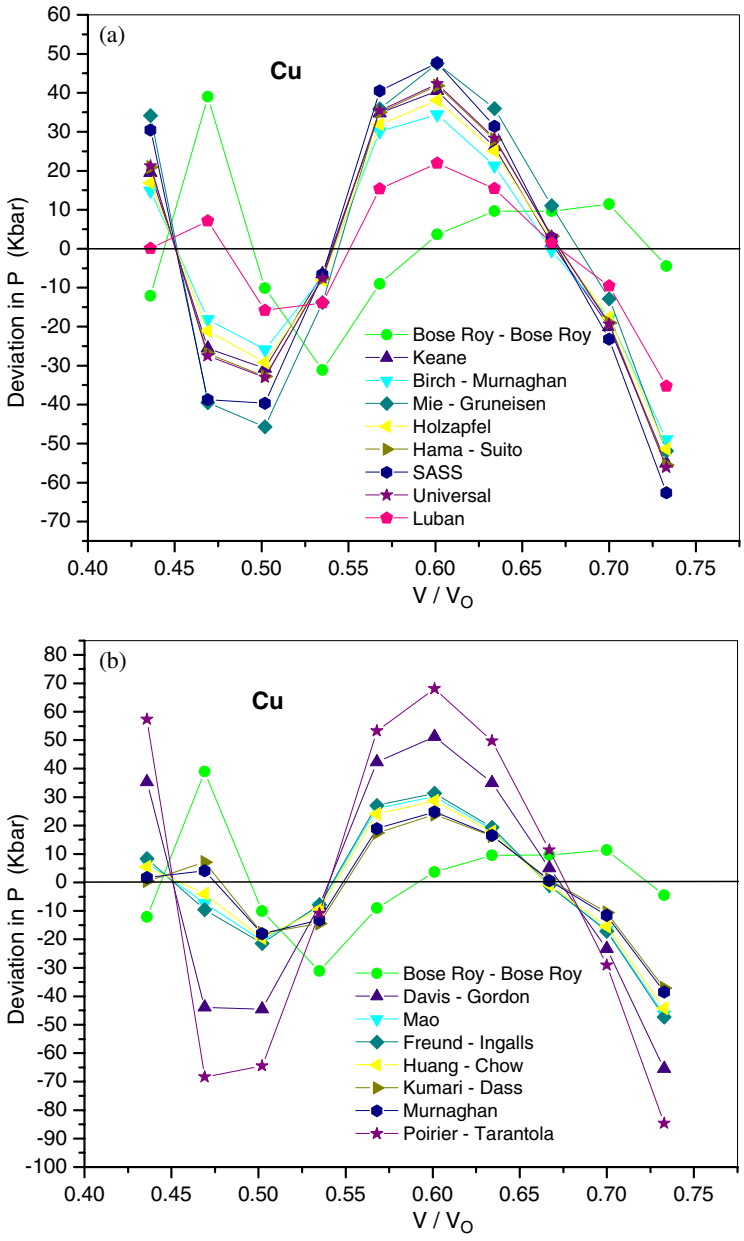

Figure 3. (a) and (b). Comparison of deviations between the data curve of Cu [58] and the fits from Bose Roy–Bose Roy, and the other equations of state.

several solids to show that the Keane equation is slightly superior to the Murnaghan equation. Macdonald [80], however, contended that a small difference between the B_0' values used in data fitting with the Keane equation and with the Murnaghan equation would render the resulting curves the same within the likely experimental error of the data used by Anderson. Although the Keane EOS is better, the difference between the two EOSs, as noted earlier, is not large. In fact, by arbitrarily using slightly different values of B_0', the predictions of many such equations

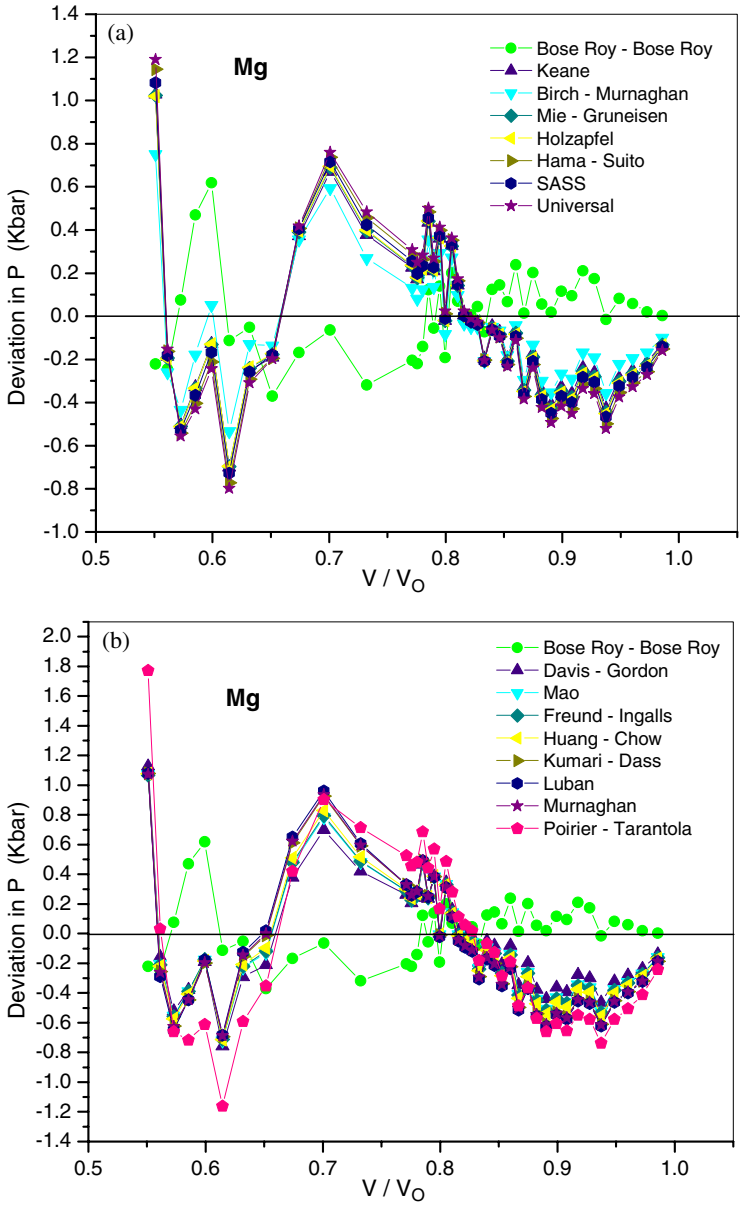

Figure 4. (a) and (b). Comparison of deviations between the data curve of Mg [56] and the fits from Bose Roy–Bose Roy, and the other equations of state.

may be forced to converge within the desired limit of experimental uncertainty. However, the moot point is that such arbitrary exercises are unjustified for discrimination purposes, and therefore negate such contentions.

Hama and Suito [34] have compared prediction capability of some EOSs, using the theoretical values of bulk moduli parameters for some solids, including Cu, with the theoretical isotherms—and concluded that the universal EOS is in good agreement with the theoretical isotherms up to about $V/V_0 = 0.2$–0.3 or up to about 10 TPa in pressure. It is not clear

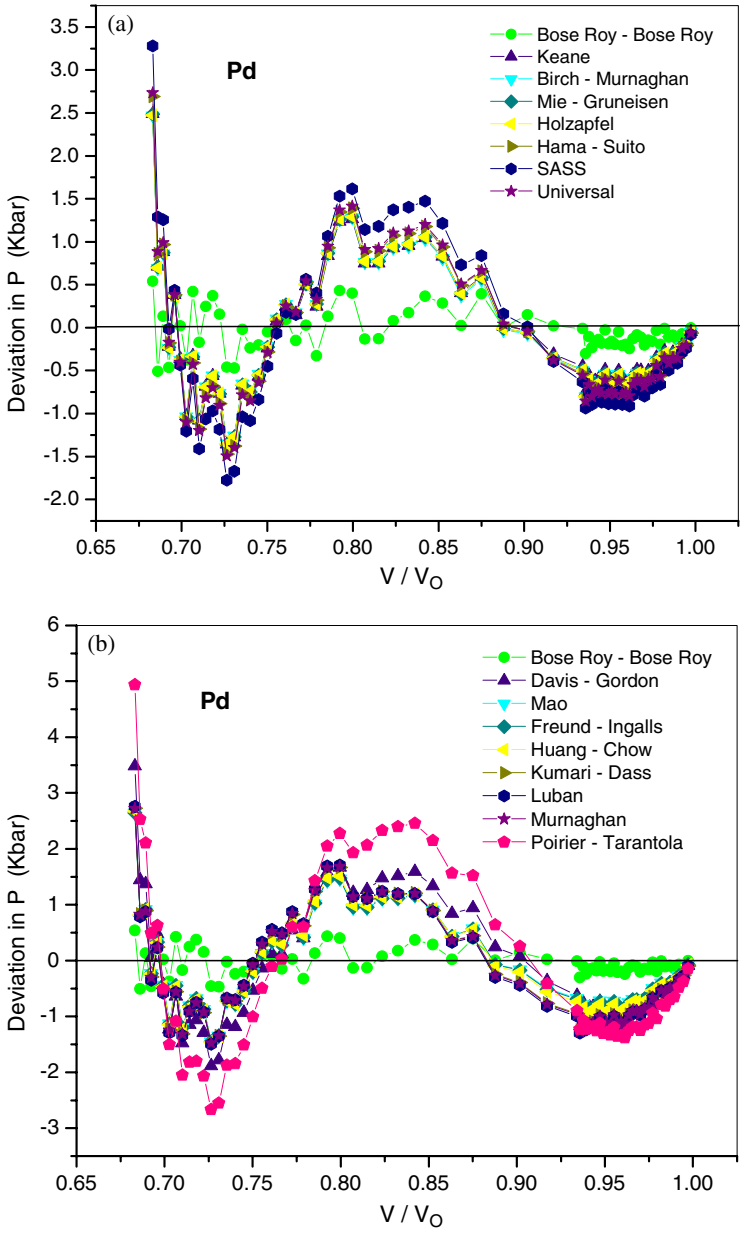

Figure 5. (a) and (b). Comparison of deviations between the data curve of Pd [56] and the fits from Bose Roy–Bose Roy, and the other equations of state.

what issues their study, involving the comparison of one theory with the other, addresses, because the test ground for the validity of an EOS is its agreement with experiment. In fact, the universal EOS badly fails (tables 4–8) to describe the experimental isotherm of Cu of Nellis *et al* [58], ranging to about 1 TPa only. Attempts to theoretically predict the EOS of solids continue [74, 75], but they are eventually guided by experiment, to check and thereby improve upon the assumptions and approximations entailed therein. Further, an EOS is required to be

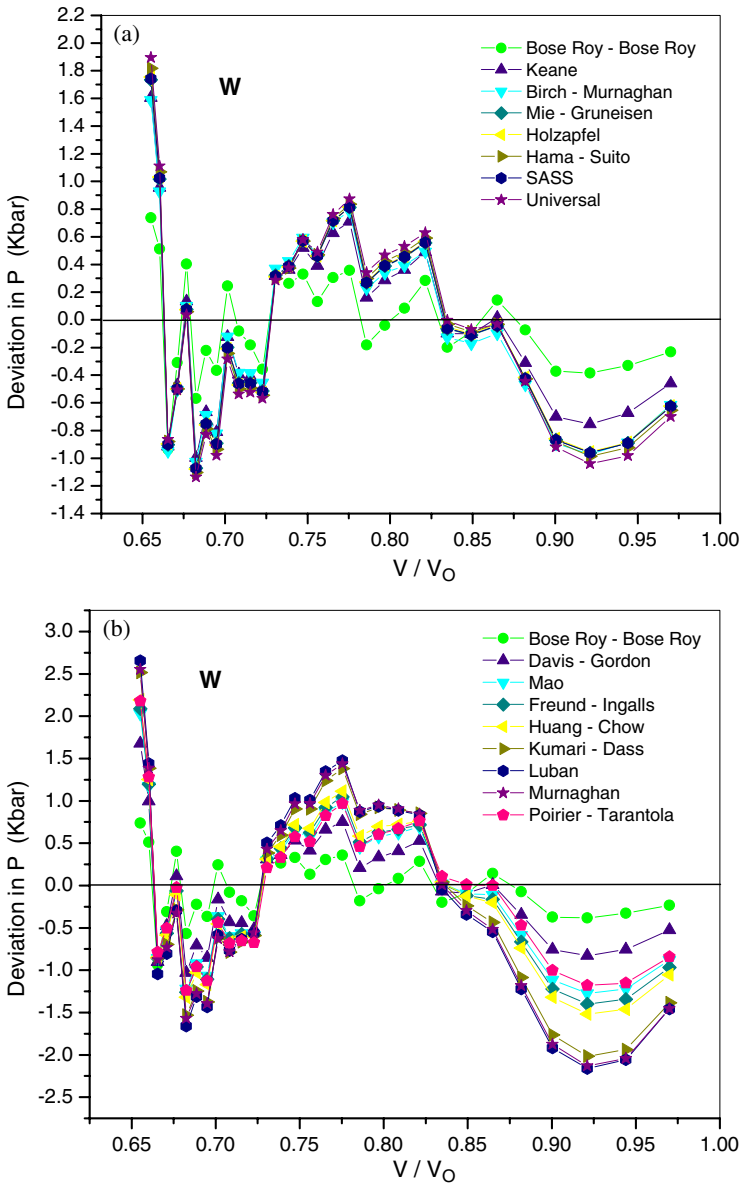

Figure 6. (a) and (b). Comparison of deviations between the data curve of W [59] and the fits from Bose Roy–Bose Roy, and the other equations of state.

applicable in practice, and also in principle [54], to the point of structural phase transition only, and not to the enormous pressure ranges theoretically conceivable. However, their improved version of the universal EOS does exhibit a better curve-fitting capability for the experimental isotherms (table 10).

The Mie–Gruneisen EOS may not have agreed well with the geophysical data [41], but the response of this EOS, based on the century-old potential, towards the laboratory compression data is noteworthy—occupying as high as the fourth position on the scale of relative utility.

Notably, the assertion of Sushil *et al* [39] that their EOS (SASS), based on a modified Eulerian strain, is better than the Birch–Murnaghan EOS is negated on experimental grounds. Further, it will be interesting to note that the Poirier and Tarantola EOS, with its claim of stronger convergence than the Birch–Murnaghan EOS refuted [85], is the poorest among all the EOSs collated in table 10. Furthermore, on fitting to the ultra-high pressure isotherm of Cu, it yields an absurd negative fit value for B_0'. Of the five outliers, equations (17)–(21), for which no results are shown, the Lagrangian EOS yields negative values for B_0' for the HPIs of Ag, Cu, and Mg, while the Slater EOS also suffers from the same limitations, yielding negative values for B_0' for as many as seven solids, excepting the rather low compression isotherms of MgO and NaCl, as anticipated by Stacey *et al* [21]. Although the fitting capability of equations (17), (19), and (20) is very poor and the fit parameters are far off from the experimental values, they do not yield such absurd negative values. Thus the Lagrangian EOS is not a mere case of a poor convergence implying a poor fitting capability [73]. However, we have observed no such absurd behaviour for any of these outliers for the LPIs. Obviously, these EOSs were considered viable because they could fit well the then achievable EOS data, ranging to low pressures.

4. Summary

A most stringent discrimination technique, comprising seven separate tests, is applied to all the isothermal three-parameter EOSs—with reference to nine model-independent and accurate isotherms with pressures/compressions ranging to very high values. Although none of the seven tests is singularly sufficient to assess the adequacy of an EOS, a higher fitting accuracy in conjunction with a higher number of wiggles of the data deviation curves about the fits may provide a good guess as to the adequacy of an EOS. It is remarkable that, out of the 63 test points accompanying each of the nearest rival equations, the Keane and Birch–Murnaghan equations (tables 3–9), only one test point of each of them proves better than ours. Obviously, the accepted position in the literature that 'the Birch-Murnagan EOS is now empirically the best' [88], is not correct. Further, it is shown by numerical as well as graphical results that the difference in the curve-fitting capability of the EOSs, including the most widely used Birch–Murnaghan EOS; is not as large as the difference between them and our EOS. To conclude, an equation of state of solids continues to be invoked as an interpolation and smoothing device for the data, and for the extraction of accurate values of bulk modulus values from them. Analysis of curve-fitting results clearly indicates that while most of the EOSs lie in a narrow band of utility for these purposes, our model on an overall assay—with its excellent fitting capability for quantum solids of bulk modulus value of as low as $B_0 = 1.7$ kbar [36], and excellent fitting capability features for a broad class of materials [37]—is decisively superior to all the isothermal three-parameter equations of state of solids thus far proposed in the literature.

Acknowledgment

We are grateful to Professor Bertil Sundqvist, Department of Experimental Physics, Umea University, Sweden, for helping us find some references.

References

[1] Tait P G 1888 *Physics and Chemistry of the Voyage of H.M.S. Challenger* vol 2, part 4 (London: HMSO)
[2] Dymond J H and Malhotra R 1988 *Int. J. Thermophys.* **9** 941
[3] Murnaghan F D 1937 *Am. J. Math.* **59** 235
[4] Murnaghan F D 1944 *Proc. Natl Acad. Sci. USA* **30** 244

[5] Murnaghan F D 1951 *Finite Deformation of an Elastic Solid* (New York: Wiley)
[6] Murnaghan F D 1967 *Finite Deformation of an Elastic Solid* (New York: Dover)
[7] Birch F 1938 *J. Appl. Phys.* **9** 279
[8] Birch F 1939 *Bull. Seismol. Soc. Am.* **29** 463
[9] Birch F 1947 *Phys. Rev.* **71** 809
[10] Birch F 1952 *J. Geophys. Res.* **57** 227
[11] Birch F 1978 *J. Geophys. Res.* **83** 1257
[12] Slater J C 1939 *Introduction to Chemical Physics* (New York: McGraw-Hill) p 521
[13] Keane A 1953 *Nature* **172** 117
[14] Keane A 1954 *Aust. J. Phys.* **7** 322
[15] Davis L A and Gordon R B 1967 *J. Chem. Phys.* **46** 2650
[16] Anderson O L 1968 *Phys. Earth Planet. Inter.* **1** 169
[17] Thomsen L 1970 *J. Phys. Chem. Solids* **31** 2003
[18] Mao N H 1970 *J. Geophys. Res.* **75** 7508
[19] Grover R, Getting C and Kennedy G C 1973 *Phys. Rev.* B **7** 567
[20] Huang Y K and Chow C Y 1974 *J. Phys. D: Appl. Phys.* **7** 2021
[21] Stacey F D, Brennan B J and Irvine R D 1981 *Geophys. Surv.* **4** 189
[22] Anderson M S and Swenson C A 1983 *Phys. Rev.* B **28** 5395
[23] Rose J H, Smith J R, Guinea F and Ferrante J 1984 *Phys. Rev.* B **29** 2963
[24] Vinet P, Ferrante J, Smith J R and Rose J H 1986 *J. Phys. C: Solid State Phys.* **19** L467
[25] Fang Z H 1998 *Phys. Rev.* B **58** 20
[26] Dodson B W 1987 *Phys. Rev.* B **35** 2619
[27] Sikka S K 1988 *Phys. Rev.* B **38** 8463
[28] Freund J and Ingalls R 1989 *J. Phys. Chem. Solids* **51** 263
[29] Kumari M and Dass N 1990 *J. Phys.: Condens. Matter* **2** 3219
[30] Holzapfel W B 1991 *Europhys. Lett.* **16** 67
[31] Parsafar G and Mason E A 1994 *Phys. Rev.* B **49** 3049
[32] Baonza V G, Caceres M and Nunez Z 1995 *Phys. Rev.* B **51** 28
[33] Holzapfel W B 1996 *Rep. Prog. Phys.* **59** 29
[34] Hama J and Suito K 1996 *J. Phys.: Condens. Matter* **8** 67
[35] Poirier J P and Tarantola A 1998 *Phys. Earth Planet. Inter.* **109** 1
[36] Bose Roy S and Bose Roy P 1999 *J. Phys.: Condens. Matter* **11** 10375
[37] Bose Roy P and Bose Roy S 2003 *J. Phys.: Condens. Matter* **15** 1643
[38] Deng X Q and Yan Z T 2002 *High Temp.—High Pressures* **34** 387
[39] Sushil K, Arunesh K, Singh P K and Sharma B S 2004 *Physica* B **352** 134
[40] Saxena S K 2004 *J. Phys. Chem. Solids* **65** 1561
[41] Stacey F D and Davis P M 2004 *Phys. Earth Planet. Inter.* **142** 137
[42] Ponkratz U and Holzapfel W B 2004 *J. Phys.: Condens. Matter* **16** S963
[43] Sun J X, Wu Q, Cai L C and Jing F Q 2005 *J. Phys. Chem. Solids* **66** 773
[44] Sun J X 2005 *J. Phys.: Condens. Matter* **17** L103
[45] Hofmeister A M 1991 *J. Geophys. Res.* **96** 21893
[46] Birch F 1986 *J. Geophys. Res.* **91** 4949
[47] Schlosser H 1993 *Phys. Rev.* B **48** 6646
[48] Kim H S, Graham E K and Voigt D E 1989 *Trans. Am. Geophys. Union* **70** 1368
[49] Spetzler H, Sammis C G and O' Connell R J 1972 *J. Phys. Chem. Solids* **33** 1727
[50] Anderson O L 1995 *Equations of State of Solids for Geophysical and Ceramic Science* (New York: Oxford University Press)
[51] Macdonald J R and Powell D R 1971 *J. Res. Natl Bur. Stand.* A **75** 441
[52] Schlosser H and Ferrante J 1988 *Phys. Rev.* B **37** 4351
[53] Sato Y 1977 *High-Pressure Research: Applications in Geophysics* ed M H Manghani and S Akimoto (San Diego, CA: Academic) p 307
[54] Angel R J and Ross N L 1996 *Phil. Trans. R. Soc.* A **354** 1449
[55] Mathews J H 1994 *Numerical Methods for Mathematics, Science, and Engineering* 2nd edn (New Delhi: Prentice-Hall of India) p 278
[56] Carter W J, Marsh S P, Fritz J N and McQueen R G 1971 *Accurate Characterization of the High Pressure Environment* Special Publication No 326, ed E C Lyod (Washington, DC: US Government Printing Office) p 147

[57] Fritz J N, Marsh S P, Carter W J and McQueen R G 1971 *Accurate Characterization of the High Pressure Environment* Special Publication No 326, ed E C Lyod (Washington, DC: US Government Printing Office) p 201
[58] Nellis W J, Moriarty J A, Mitchell A C, Ross M, Dandrea R G, Aschcroft N W, Holmes N C and Gathers G R 1988 *Phys. Rev. Lett.* **60** 1414
[59] Hixson R S and Fritz J N 1992 *J. Appl. Phys.* **71** 1721
[60] Freund J and Ingalls R 1989 *Phys. Rev.* B **39** 12537
[61] Simmons G and Wang H 1971 *Single Crystal Elastic Constants and Calculated Aggregate Properties* 2nd edn (Cambridge: MIT)
[62] Kittel C 1976 *Introduction to Solid State Physics* 5th edn (New York: Wiley)
[63] Ullmann W and Pan'kov V L 1976 *Zentralinstitut fur Physik der Erde, Potsdam*
[64] Greene R G, Luo H and Ruoff A L 1994 *Phys. Rev. Lett.* **73** 2075
[65] Swenson C A 1968 *J. Phys. Chem. Solids* **29** 1337
[66] Vant't Klooster P, Traphenters N J and Biswas S N 1979 *Physica* B **97** 65
[67] Anderson O L 1966 *J. Phys. Chem. Solids* **27** 547
[68] Holzapfel W B 1997 *High-Pressure Techniques in Chemistry and Physics* ed W B Holzapfel and N S Isaacs (New York: Oxford University Press) p 47
[69] Wang K and Reeber R R 1997 *High Temp. Mater. Sci.* **36** 185
[70] Jeanloz R 1992 *High Pressure Research in Geophysics* ed M H Manghnani and S Akimoto (Tokyo: Center of Academic Publications) p 147
[71] Mao H K and Bell P M 1979 *J. Geophys. Res.* **84** 4533
[72] Anderson O L and Andreatch P Jr 1966 *J. Am. Ceram. Soc.* **49** 404
[73] Barch G R and Chang Z P 1971 *Accurate Characterization of the High Pressure Environment* Special Publication NBS Circular no 326, ed E C Lyod (Washington, DC: US Government Printing Office) p 173
[74] Chisolm E D, Crockett S D and Wallace D C 2003 *Phys. Rev.* B **68** 104103
[75] Luo S N, Swift D C, Mulford R N, Drummond N D and Ackland G J 2004 *J. Phys.: Condens. Matter* **16** 5435
[76] Hanfland M, Loa I and Syassen K 2002 *Phys. Rev.* B **65** 184109
[77] Kunc K, Loa I and Syassen K 2003 *Phys. Rev.* B **68** 094107
[78] Stacey F D 2001 *Phys. Earth Planet. Inter.* **128** 179
[79] Partington J R 1957 *An Advanced Treatise on Physical Chemistry* vol 3 (London: Longmans) p 345
[80] Macdonald J R 1969 *Rev. Mod. Phys.* **41** 316
[81] Katahara K W, Manghnani M H, Ling L C and Fisher E S 1997 *High Pressure Research Applications in Geophysics* ed M H Manghnani and S Akimoto (New York: Academic) p 351
[82] Lundqvist B I, Bogicevic A, Carling K, Dudiy S V, Gao S, Hartford J, Hyldgaard P, Jacobson N, Langreth D C, Lorente N, Ovesson S, Razaznejad B and Yourdshahyan Y 2001 *Surf. Sci.* **493** 253
[83] Ziambaras E and Scroder E 2003 *Phys. Rev.* B **68** 064112
[84] Yourdshahyan Y, Ruberto C, Bengtsson L and Lundqvist B I 1997 *Phys. Rev.* B **56** 8553
[85] Gaurav S, Sharma B S, Sharma S B and Upadhyaya S C 2002 *Physica* B **322** 328
[86] Hayard A T J 1967 *Br. J. Appl. Phys.* **18** 965
[87] Span R and Wagner W 1997 *Int. J. Thermophys.* **18** 1415
[88] He D, Zhao Y, Daemen L L, Qian J, Lokshin K, Shen T D and Zhang J 2004 *J. Appl. Phys.* **95** 4645